Star polymers: study of fluid–fluid transitions in a system with a repulsive ultrasoft-core

2003 J. Phys.: Condens. Matter 15 1505

(http://iopscience.iop.org/0953-8984/15/10/301)

INSTITUTE OF PHYSICS PUBLISHING JOURNAL OF PHYSICS: CONDENSED MATTER

J. Phys.: Condens. Matter **15** (2003) 1505–1520 PII: S0953-8984(03)53626-8

Star polymers: study of fluid–fluid transitions in a system with a repulsive ultrasoft-core

F Lo Verso[1], M Tau[2] and L Reatto[1]

[1] Istituto Nazionale di Fisica della Materia and Dipartimento di Fisica, Universitá di Milano, Via Celoria 16, Milano, Italy
[2] Istituto Nazionale di Fisica della Materia and Dipartimento di Fisica, Universitá di Parma, Via Universitá 12, Parma, Italy

E-mail: federica.loverso@mi.infn.it

Received 18 September 2002
Published 3 March 2003
Online at stacks.iop.org/JPhysCM/15/1505

Abstract

We study a model for star polymers in solution which, in addition to the ultrasoft repulsive interaction of entropic origin, has an attractive interpolymer interaction at longer range. This attraction can arise from a suitable tuning of the solvent and solute properties.

For this model we study the phase diagram using mean-field theory and two fluid-state theories, the modified hypernetted chain (MHNC) integral equation and the hierarchical reference theory, and we explore star polymers with a different number of arms f ($f = 12, 24, 32, 40$). All three theories give the same topology for the phase diagram in the presence of attraction. When the strength of the interaction is strong enough a fluid–fluid phase transition appears but the coexistence curve in the density–temperature (strength of attraction) bifurcates at a triple point into two lines of coexistence terminating at two critical points. This peculiar phase behaviour is related to the unusual form of the repulsive contribution $V_{rep}(r)$: at low density and in a semidilute regime the soft-core Yukawa-like part of $V_{rep}(r)$ is relevant, at higher densities the logarithmic, ultrasoft part of $V_{rep}(r)$ is the relevant one.

During our study we verify that the MHNC equation also gives a very accurate description of correlations for systems with an ultrasoft-core potential.

1. Introduction

In the last decades theoretical and experimental interest in the structure, dynamics and thermodynamical behaviour of colloidal suspensions has grown. To study such systems a general approach is to trace out some of the degrees of freedom, like the ones of the solvent, thus leaving an effective interaction between the remaining ones, those of the centre of mass of the macroparticles. Very different colloidal solutions can actually be well synthesized whose

interaction, tunable through experimental control of particle and solvent properties, can be modelled by a simple, effective pair interaction $V(r)$. $V(r)$ is, in general, state dependent and, in addition, its dependence on r can be rather different from the one typical of a simple molecular system [1]. An example is the presence of a very deep and narrow attractive well outside a repulsive core that one finds with the depletion interaction.

In more recent years it has been pointed out that the short range repulsive part of $V(r)$ can also be very different, or almost so, from the hard core which is present in simple atomic systems. This is the case for the effective interaction between the centres of mass of two macromolecules in a good solvent, as the case of dendrimers [2, 3] and of the linear polymers [4] in which $V(r)$ does not diverge at all at the origin but reaches a finite value that can be of the order of the thermal energy.

Another relevant case is that of star polymers in a good solvent. Solutions of star polymers have recently received attention both from the theoretical [5–8] and the experimental point of view [9–12], as very soft colloidal particles. The mutual star–polymer interaction, in a good solvent, is entropic in origin; $V(r)$ diverges at small r, at least in some simple modelization of the entropic interaction, but $V(r)$ increases very slowly as the distance r between a pair of star polymers decreases, that is in a logarithmic way. This potential has been called ultrasoft. The strength of this interaction depends on the number f of arms of the star polymer, roughly increasing as $f^{3/2}$ [5]. This system is an interesting example of a complex fluid for which the phase diagram has special features arising from the ultrasoft nature of the effective interaction $V(r)$. In fact for $f < 34$ the system is fluid at all concentrations, whereas for $f \geqslant 34$ the system is fluid at low and at large concentrations but crystalline phases appear at intermediate concentrations [7]. Since $V(r)$ has an entropic origin the system is athermal, i.e. the phase diagram does not depend on temperature.

In a real solution of star polymers other interaction terms can be present in addition to the previous entropic contribution. Some residual dispersion forces can be present thus giving rise to interpolymer attraction and its intensity can be controlled by modifying the solvent. It should be possible to induce attractive depletion forces by adding to the solution an additional component of small size compared to the star polymer but large compared to the solvent molecules. We might expect that when the intensity of these attractive forces is sufficiently large, some sort of fluid–fluid phase transition will arise, similar to the liquid–vapour phase transition in a simple fluid, but to what extent the phase diagram is modified by the presence of the ultrasoft core is not known. It is the purpose of this paper to investigate the phase diagram of a solution of star polymers with attraction, and search for the presence of fluid–fluid phase transitions on the basis of different liquid state theories.

First we study the phase diagram by applying a mean-field theory. This is a very simple scheme, yet it is useful in order to give some general insight into the phase behaviour concerning the fluid–fluid phase transition. Second we apply the integral equation method which builds the thermodynamic properties from the radial distribution function $g(r)$.

In the case of the purely repulsive star–star interaction the Rogers–Young (RY) equation [13] has been used with success [6]. However, in the case of simple fluids, it is known that the RY equation is not as accurate as in the case of attractive forces [14, 15], so we have adopted the modified hypernetted chain (MHNC) equation which is also accurate when the attraction is present [16].

We tested the accuracy of the MHNC equation in the case of the purely repulsive ultrasoft potential. Over the full range of density of interest our results show that the MHNC equation is an excellent tool for studying this ultrasoft potential, and actually it is more accurate than the RY equation. Then we introduced a simple model for the attractive contribution to the effective interaction and we analysed the presence of such fluid–fluid transition with MHNC

closure. As a third theory we used the hierarchical reference theory (HRT) [17, 18], which incorporates in the liquid state theory the renormalization-group (RG) treatment of the critical fluctuations.

All three theoretical approaches give the same topology for the phase diagram: if the number of arms is not too large (we have investigated in detail $f = 24$ and 32), so that no crystalline phases are present for the densities of interest, the system has two lines of fluid–fluid phase transition with two critical points and a triple point. The coexistence line at lower concentration is similar to the liquid–vapour transition in a simple fluid. The second coexistence line is specific to this ultrasoft system and it is present in the region of large concentration where there is a strong overlap of the stars. For a larger number of arms the low density fluid–fluid transition persists but the second line of fluid–fluid transition is suppressed by freezing for $f \gtrsim 50$. In the intermediate range ($34 \lesssim f \lesssim 50$) the triple point is suppressed by freezing whereas the two critical points persist. Our work is organized as follows: in section 2 we study the system on the basis of mean field. In section 3 we introduce a specific model for the attraction and the theories for correlations we are using (MHNC and HRT). The results for the phase diagram and correlation functions are summarized in section 4. Section 5 contains our conclusions. In the appendix we apply MHNC to the case of the purely repulsive interaction and we compare the results with simulation and with RY ones [6].

2. Introduction of the reference system and mean-field analysis

The effective pair interaction between star polymers with f arms in a good solvent is purely repulsive and for $f \geqslant 10$ it reads as follows:

$$\frac{V_{rep}(r)}{k_BT} = \frac{5}{18} f^{\frac{3}{2}} \left[-\ln\left(\frac{r}{\sigma}\right) + \left(1 + \frac{\sqrt{f}}{2}\right)^{-1} \right] \qquad (r \leqslant \sigma) \tag{1}$$

$$= \frac{5}{18} f^{\frac{3}{2}} \left(1 + \frac{\sqrt{f}}{2}\right)^{-1} \left(\frac{\sigma}{r}\right) \exp\left[\frac{-\sqrt{f}(r-\sigma)}{2\sigma}\right] \qquad (r > \sigma) \tag{2}$$

σ is the corona diameter of the star and measures the extension of the star (Daoud–Cotton model for the conformation of star polymers [19]). The value of σ depends on the number N of monomers in a single arm. For very long chains and in good solvents it reads

$$\sigma \propto m N^{\frac{3}{5}} f^{\frac{1}{5}} \left(\frac{v}{m^3}\right)^{\frac{1}{5}} \qquad N \gg f^{\frac{1}{2}} \left(\frac{m^3}{v}\right)^2 \tag{3}$$

where m is the linear extension of a monomer and v denotes the excluded volume interaction parameter which has the dimension of a volume.

This form of the interaction has been derived by scaling theory [5] for $r < \sigma$ and for $r > \sigma$ it is a convenient analytical form which has been shown [12], for an ample range of f values, to give a good description of small angle neutron scattering (SANS) results on concentrated star polymer samples. This form is further confirmed by microscopic molecular dynamics (MD) simulations of star polymers with up to $f = 50$. When $f \leqslant 10$ the Yukawa form equation (2) is no longer accurate [20] but we do not study here stars with such a small number of arms.

This effective interaction is entropic in origin so that $V_{rep}(r)/T$ is independent of the temperature, i.e. the system is athermal. $V_{rep}(r)$ diverges at $r = 0$ but it increases as $r \to 0$ very slowly, in a logarithmic way, and for this reason it has been called an ultrasoft potential to distinguish it from the potentials appropriate for atomic fluids.

In view of the studies described below we need to know the properties of the reference system, i.e. the system interacting with $V(r)_{rep}$. We have studied the thermodynamics and

the structural properties relating to the fluid phase of star polymers solution modelled by pair interaction (1), (2) with the MHNC equation. The thermodynamic quantities relevant to the description of the phase behaviour can be deduced from a structural function which measures the degree of correlation between pairs of particles as the radial distribution function $g(r)$. In particular we have used the isothermal compressibility as given by the structure factor $S(q)$ at $q = 0$ to construct the equation of state.

The MHNC integral equation is based on approximating the so-called bridge function of a system with potential $V(r)$ by the bridge function of the hard spheres fluid of suitable diameter and a variational principle fixes this diameter [21]. It is known that the MHNC is very accurate for a wide range of shapes of the interatomic potential $V(r)$, and also when $V(r)$ has an attractive part. Recently the universality of the hard sphere bridge function has been verified for a system of penetrable spheres and inferred for a bounded potential with high penetrability [22].

We have verified that the MHNC equation gives a very accurate description of the thermodynamic and of the correlation function of a system interacting with the potential (1), (2) over all values of density and f values of our computations; the results of this study can be found in the appendix. The MHNC follows accurately the result of the simulation and reproduces the peculiar behaviour that the short range order, as measured by the height of the peaks of $g(r)$, first increases for increasing density ρ of the star polymers, but at a certain point there is a changeover and correlations decrease for increasing density until a further changeover is encountered at still larger values of ρ.

Over a large part of the density range the RY equation and the MHNC equation have comparable accuracy and both give results in very good agreement with simulation. The accuracy of the MHNC also remains very good in the ranges of density of strongest coupling (this corresponds to the regions where the effective hard sphere packing fraction has a maximum, see figure 5) where RY is not as accurate.

As mentioned in the introduction we should expect that under certain conditions the effective interaction between two star polymers contains a additional contribution $w(r)$ to be added to the repulsive part $V_{rep}(r)$ of equations (1) and (2):

$$V_{tot}(r) = V_{rep}(r) + w(r). \tag{4}$$

We consider the case of an attractive $w(r)$. This attraction could be due to a van der Waals interaction arising from a nonperfect matching of the refraction index of the solvent and of the polymer in such a way that this does not alter the basic configuration of the single star polymer.

Another source of attraction is a depletion interaction when in the solution a third component is present which is large compared with the solvent molecules but small compared with the star polymers. If the intensity of the attraction becomes large enough we should expect the presence of a fluid–fluid transition. If $w(r)$ is independent of temperature as we assume here, this condition is achieved if the temperature is low enough. In the case where $w(r)$ has an entropic origin, so that $w(r)$ is also proportional to T, it will be necessary to change some other control parameter, such as depletant size and concentration, in order to increase the strength of $w(r)$ and reach the condition for a phase transition. In what follows we shall use temperature as a control parameter.

First of all, to analyse and characterize the possibility of a fluid–fluid phase transition we utilized a mean-field (MF) theory, a useful approximation in order to get at least a qualitative picture of the phase diagram. For this purpose we have used the information about thermodynamical properties of the reference system (the repulsive star–star interaction V_{rep}) as found with the MHNC equation. Within MF the specific analytic form of $w(r)$ does not enter, only its integrated intensity. In fact within such approximation the free energy of a

Table 1. Critical temperatures and densities for different f values for MF results. The last column contains T_{inst}, the temperatures below which we found mechanical instability (see section 2).

f	ρ^*_{c1}	T^*_{c1}	ρ^*_{c2}	T^*_{c2}	T_{inst}
40	0.046	0.6846	1.900	0.1970	0.1942
32	0.047	0.6722	1.960	0.2469	0.2422
24	0.050	0.6700	1.920	0.3267	0.3225
12	0.078	0.7463	1.400	0.6054	0.6050

system can be written as:

$$\frac{A}{V} = f_{ref} - \rho^2 a \tag{5}$$

where f_{ref} is the free energy density due to the repulsive part V_{rep} of the potential, ρ is the number density of the macroparticles and

$$a = -\tfrac{1}{2}\int w(\boldsymbol{r})\,\mathrm{d}\boldsymbol{r}. \tag{6}$$

First we look for the presence of critical points, i.e. we search for solutions of the following equations:

$$\left.\frac{\partial^2 f_{ref}}{\partial\rho^2}\right|_{T=T_c} - 2a = 0 \tag{7}$$

$$\left.\frac{\partial^3 f_{ref}}{\partial\rho^3}\right|_{T=T_c} = 0. \tag{8}$$

The thermodynamics of the reference system is obtained via the compressibility relation which can be written in the form

$$\left(\frac{\partial^2 f_{ref}}{\partial\rho^2}\right) = \frac{1}{\beta\rho S(0,\rho)_{ref}} \tag{9}$$

where $\beta = (k_B T)^{-1}\partial^3 f_{ref}/\partial\rho^3$ is obtained by an additional density derivative of the right-hand side of equation (9). In turns out that equation (8) has three solutions: two are significant, let us call them ρ^*_{c1} and ρ^*_{c2}, and the third is not significant because it corresponds to a temperature for which, as we will see below, our model presents a mechanical instability. Note that in the case of hard spheres, for instance, equation (8) has only one solution. ρ^*_{c1} and ρ^*_{c2} depend on the number f of arms and table 1 contains the values of the critical densities for a few values of f. We indicate with (*) the reduced quantities of interest in our study ($\rho^* = \rho\sigma^3$, $T^* = k_B T C^{-1}$ and, in the following, $P^* = PC^{-1}$, $a^* = aC^{-1}\sigma^{-3}$, where C represents the amplitude of the attractive contribution[3], see next section). From equations (7) and (9) one gets the critical temperature:

$$k_B T_c = 2a\rho_c S(0,\rho_c)_{ref}. \tag{10}$$

In figure 1 we show some of the isotherms around the two critical temperatures for $f = 32$. We note, around the critical densities, a *plateau* corresponding to T^*_{c1} and T^*_{c2} and we see the typical van der Waals loop for $T^* < T^*_{c1}$ and $T^* < T^*_{c2}$. The spinodal curves are obtained as the loci of vanishing $\partial^2 f_{ref}/\partial\rho^2$ and are shown in figure 2 for $f = 32$. In order to determine the coexistence pressure we studied the behaviour of the reduced chemical potential versus P^* for $T^* < T^*_{c1}$ and $T^* < T^*_{c2}$. The intersection between the high and low density branches of

[3] In our specific case the attractive contribution is $w(r) = -C\,(\exp[(r-A)/B]+1)^{-1}$.

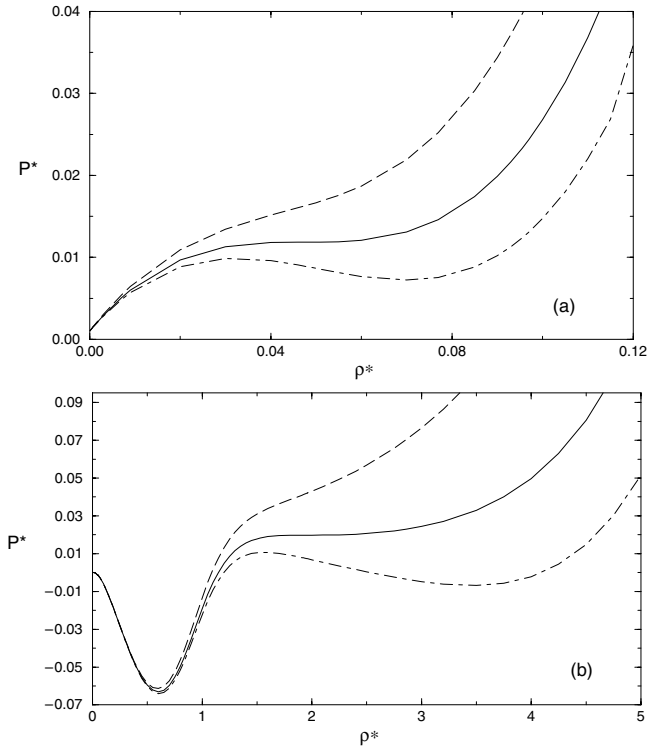

Figure 1. (a) Reduced pressure $P^* = PC^{-1}$ versus reduced density $\rho^* = \rho\sigma^3$ for a potential with a repulsive ultrasoft core ($f = 32$). Long dashed curve, solid curve, dot–dashed curve stand for the supercritical ($T^* = 0.7167$), critical ($T^* = T^*_{c1} = 0.6722$) and subcritical ($T^* = 0.6425$) isotherm respectively. The data has been obtained through a mean-field calculation. (b) Same as (a) but the isotherms and the density region investigated are around $T^* = T^*_{c2} = 0.2469$ (solid curve) and $\rho^* = \rho^*_{c2}$ respectively. Long dashed curve and dot–dashed curve stand for $T^* = 0.2484$ and 0.2461 respectively.

the curve for fixed T^*, verifies the condition of thermal, mechanical and chemical equilibrium between the two coexisting phases and the results for $f = 32$ and 24 are shown in figures 3 and 4 respectively. It should be noticed that for $f = 24$ the second critical point is metastable. This point, and the relative region of coexistence of phase, fall below the coexistence curve corresponding to the low density critical point. These results will be modified with the more accurate HRT study of the next section which gives two phase transitions corresponding to stable states.

It should be noted that our model has a mechanical instability toward collapse at a low enough temperature. Such behaviour can be understood by writing the reduced pressure in the form

$$P^* = T^* \int^{\rho^*} \frac{\mathrm{d}\rho^*}{S(0, \rho^*)_{ref}} - a^* \rho^{*2} \tag{11}$$

and therefore analysing the behaviour of $S(0, \rho^*)_{ref}$ as function of the reduced density[4]. In a model with strong repulsion at short distances, as appropriate for fluids of simple atoms, the inverse compressibility $S(0, \rho)^{-1}$ increases very rapidly for increasing density so that, at any

[4] We studied the behaviour of $S(0, \rho^*)_{ref}$ versus ρ^* for different values of the chains number.

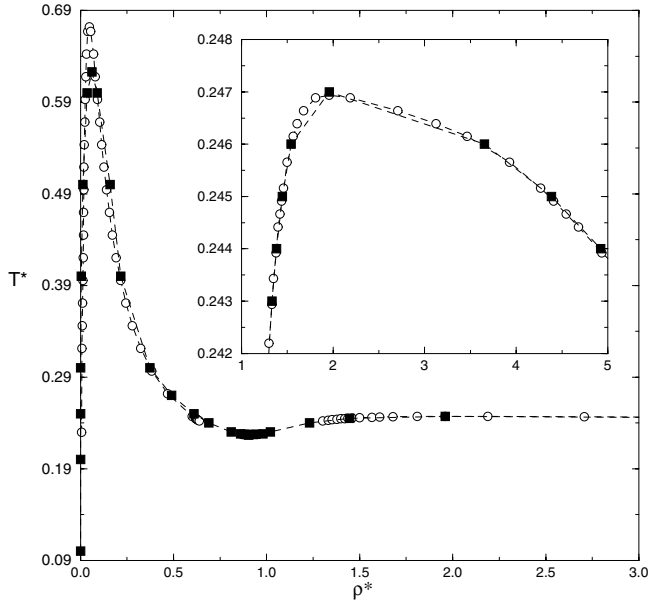

Figure 2. The spinodal curve (reduced temperature $T^* = k_B T/C$ versus reduced density $\rho^* = \rho\sigma^3$) as obtained from the MHNC approximation (squares) and numerical-MF calculation (circles) for $f = 32$, $A = 2.1\sigma$ and $B = 0.35\sigma$ (equation (12)). Main figure: low density spinodal curve and a small portion of the area around the high density critical point. Inset: high density spinodal curve; the MF curve has been drawn up to the temperature for which the pressure versus the density has physical meaning (see equation (11)). Curves are simply a guide to the eye.

finite temperature, the first contribution to the pressure in equation (11) dominates over the second contribution when the density is large enough so that the overall pressure is positive. The situation is different for the ultrasoft potential. $S(0, \rho)^{-1}$ also increases in this case for increasing density, but much more slowly. The MHNC results show that $[S(0, \rho^*)_{ref}]^{-1}$ increases approximately as the first power of ρ^* when $\rho^* \gtrsim 1$. Therefore the contribution of the repulsive forces to the pressure also increases as ρ^{*2}. As a consequence there is a value T_{inst} below which the pressure becomes negative and decreases with no bound as ρ^* increases. The value of T_{inst} depends on f and it is given in table 1.

Our analysis obtained with the MHNC equation confirms that star polymers belong to the class of the 'weak mean-field fluids', the thermodynamics of which can be accurately described by mean-field theory [23, 24]. According to our MHNC calculation in this high density limit, for $f \lesssim 40$ the coefficient of proportionality between ρ^* and $[S(0, \rho^*)_{ref}]^{-1}$ differs from the mean-field value ($\beta \int V(\boldsymbol{r})\, \mathrm{d}\boldsymbol{r}$) by less than 1%.

In summary, MF gives two lines of fluid–fluid phase transition, and the lines end at two critical points and have a triple point. However for $f = 24$ the triple point disappears since the second transition line turns out to be metastable with respect to a transition between a high density fluid and a diluted one. So only the first low density critical point is stable while the second one is metastable. The coexistence line at low density is similar to the standard liquid–vapour phase transition in the sense that the average distance between neighbouring particles is well above the characteristic size σ of the particles. The second branch is peculiar to this ultrasoft potential and, in fact, the densities of the coexisting phases are such that there is a strong overlap of the star polymers. The ratio of the two critical temperatures depends on f,

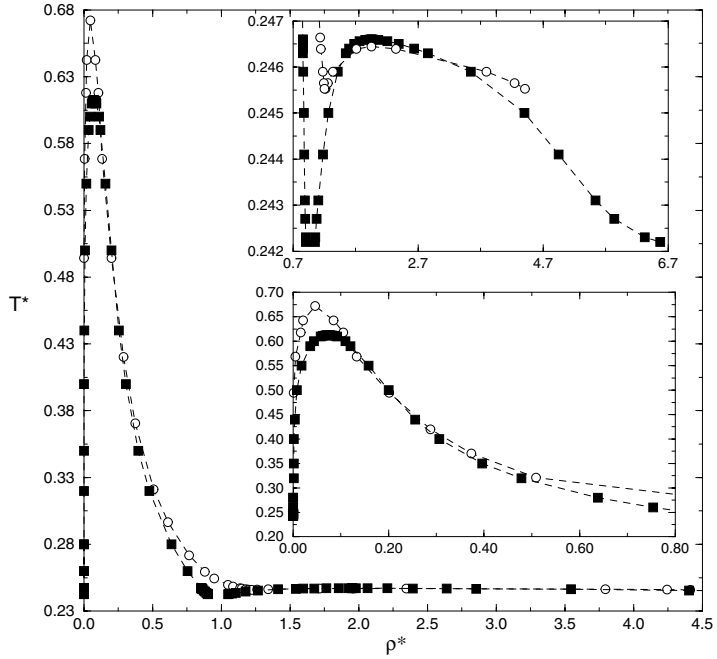

Figure 3. Coexistence curve ($f = 32$, $A = 2.1\sigma$, $B = 0.35\sigma$): MF theory (circles) and HRT theory (squares) (reduced temperature $T^* = k_B T/C$ versus reduced density $\rho^* = \rho\sigma^3$). The insets show the high density coexistence curve (bottom) and the low density one (top). Curves are simply a guide to the eye.

it is above 3 when $f = 40$ but is only 1.2 for $f = 12$. Similarly the critical densities are far apart for large f and they are closer for smaller f values. An additional feature of the second line of fluid–fluid phase transition is that its temperature range is quite narrow; T_{c2} is above the temperature of the triple point by less than 1% ($f = 32$). This range increases on the basis of more advanced theories (see the next section) but in any case it remains quite narrow. The second critical point takes place at a density where strong short range correlations are present. We have to worry then about the possible occurrence of the freezing transition. We argue that the freezing transition is not significantly modified by the presence of the attractive forces. In fact, as discussed in the next section, it turns out that these attractive forces have a minor effect on the amount of short range order in the fluid phase at the large value of density of interest. Therefore we can assume that freezing is not affected by $w(r)$. For $f \leqslant 32$ no freezing transition is present so that the lines of phase transitions represent stable states. For $f \gtrsim 50$ all the density region from the triple point to the high density critical point is covered by crystalline phases so that only the low density critical point survives as a stable state and the second critical point could only be present as a metastable state. In the intermediate region $34 \leqslant f \lesssim 50$ crystalline phases are present in a limited range of density which is located around the density of the triple point. Therefore both lines of fluid–fluid transitions and their critical points persist as stable states and only part of the coexistence curves around the triple point is pre-empted by crystallization. It would be useful to perform some simulation study in order to confirm this scenario based on the assumption that freezing is not affected at all by $w(r)$.

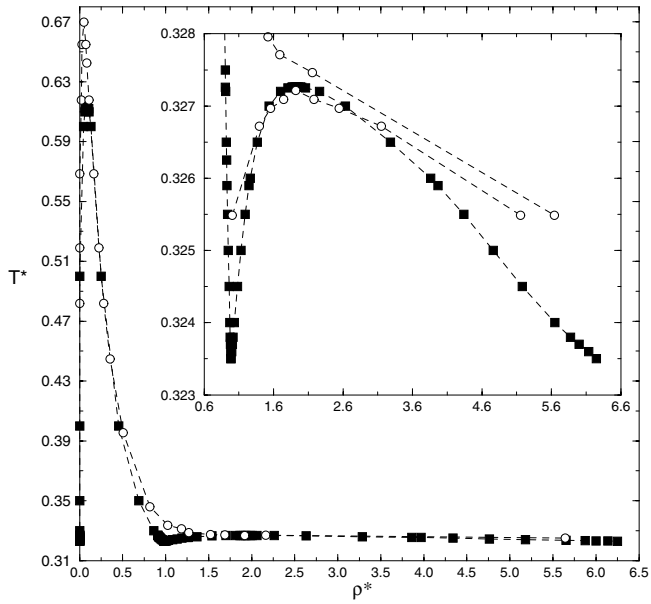

Figure 4. Coexistence curve ($f = 24$, $A = 2.1\sigma$, $B = 0.35\sigma$): MF theory (circles) and HRT theory (squares) (reduced temperature $T^* = k_B T/C$ versus reduced density $\rho^* = \rho\sigma^3$). Inset: magnifications of the high density coexistence region. We also show the MF high density curve which is metastable. Lines are simply a guide to the eye.

3. MHNC and HRT analysis

In order to obtain a more precise quantitative description of the phase diagram we have to develop a theory of correlation in the presence of the total potential. In order to do so we have to specify the form of the attractive part $w(r)$ of the potential. As discussed in the previous section, different physical mechanisms can be at the origin of the attraction. Here we are not interested in the study of one specific mechanism, but in the study of the generic features of the phase diagram so that we can use a simplified model for the attraction. We could use a square well for $w(r)$ but V_{tot} would again become repulsive at large r due to the Yukawa form of V_{rep}. We have decided to assume for $w(r)$ the functional form of a Fermi distribution, i.e.

$$w(r) = -\frac{C}{\exp\left[\frac{r-A}{B}\right]+1}. \tag{12}$$

The parameters A and B control the position and the width of the well potential and C its amplitude. By a suitable choice of these parameters one can guarantee that $V_{tot}(r)$ does not have a subsidiary maximum at large r.

As a first theory of the correlation we have used the integral MHNC equation as described in the previous section for the reference system but now the full potential $V_{tot}(r) = V_{rep}(r)+w(r)$ enters into the equation. As in the case of model potentials with attraction for atomic fluids we find that for a given ρ, the MHNC does not converge below a certain temperature $T_{sing}(\rho)$ and in its neighbourhood the isothermal compressibility has a sharp increase. This locus is assimilated to the spinodal line and the maximum of $T_{sing}(\rho)$ as function of ρ represents a critical point. The computation of the coexistence line with the MHNC is very tedious and we have not done it.

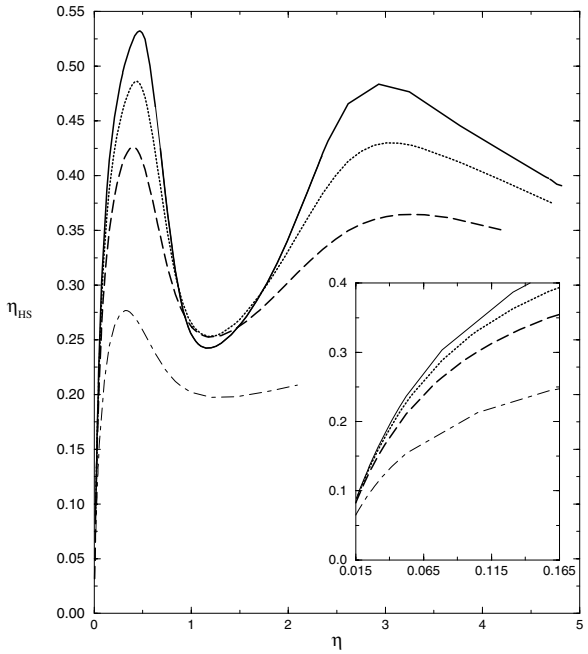

Figure 5. Effective packing fraction η_{HS} as a function of η for different values of the number of chains: dot–dashed curve, dashed curve, dotted curve, solid curve are $f = 12, 24, 32, 40$ respectively. The maxima are around the values of η for which there is a re-entrant loss of the spatial ordering of the stars. Inset: magnification of the small density region.

As a second theory of correlations we have used the HRT of fluids. This has proven to be a very accurate theory of the liquid–vapour phase transition for model interaction appropriate for atomic fluids, and it is the only theory of liquids with the qualitatively correct description of criticality. In fact HRT is a powerful scheme able to keep information on all length scales and to recover the RG results in the appropriate regime, while also describing accurately the short range correlations. In this scheme the attractive contribution to the interaction is introduced selectivity in wavevector space starting from the Fourier components of shortest wavelength. The corresponding evolution of the free energy and of the correlation functions as a function of the cut-off wavevector is described by an exact hierarchy of integro-differential equations of growing order [18]. In the implementation which has been widely used, the hierarchy is truncated at the first equation by supplementing this first equation with an approximate closure for the two-body correlation function of the partially coupled system embodying a thermodynamic consistency condition. It is important to note that the HRT also preserves the correct convexity of the free energy below the critical temperature. In this case the region of phase coexistence is directly obtained from the computation as a flat portion of the isotherm in the pressure–density plane.

HRT truncated to the first equation leads to a partial differential equation in density and, in the cut-off wavevector, also leads to solving Q for a given temperature. The theory needs as an input the chemical potential and the structure factor of the reference system, i.e. the system with interaction $V_{rep}(r)$ and these properties has been obtained by the MHNC equation as described in the appendix. HRT has been described in detail that we do not report here and the numerical procedure is the same as in [25] in which a version (HRT-SMSA) of the HRT suitable for soft-core systems has been introduced. The only specific aspect of the present

computation is the much larger range of densities in which the equation is integrated, up to $\rho\sigma^3 \simeq 7$ where as a boundary condition the random phase approximation (RPA) is used.

4. Results

With the MHNC we have studied in detail the phase diagram of our model of star polymers in solution with attraction for two values of f, $f = 32$ and 24. For the attraction $w(r)$ we have used the parameters $A = 2.1\sigma$ and $B = 0.35\sigma$. With such values of the parameters the shape of $V_{tot}(r)$ is very close to $V_{rep}(r)$ for $r < \sigma$ apart from a shift $-C$ and $V_{tot}(r)$ displays an attractive well which is centred around $r = 2\sigma$. The MHNC equation in the region of low density gives a critical point not far from the mean-field value both in temperature and in density. As in the case of a Lennard-Jones potential, MF overestimates the critical temperature compared to the MHNC and the deviation is larger in the case $f = 32$. The spinodal curve given by the MHNC is plotted in figure 2 together with the spinodal curve given by MF. There is an overall agreement, the spinodal being quite asymmetric and skewed toward large densities. In both approximations the spinodal reaches a minimum for a density $\rho^* \simeq 1$ and at larger densities there is a very shallow maximum at density $\rho^* \simeq 2$. At such high densities MF and the MHNC give very similar results, as might be expected, since many particles fall within the range of the forces. Thus the MHNC confirms the results of MF in the presence of a second critical point at high density. Similar conclusions are reached when $f = 24$. The critical temperature and density of the low density critical point has a weak dependence on the value of f whereas the critical temperature of the high density critical point has a strong dependence on f, T_{c2} being lower for the larger f.

We now discuss the results given by HRT. In this case the theory gives directly the curves of coexisting phases and the result for $f = 32$ is compared to the MF result in figure 3. The effect of fluctuations as embodied in HRT has the effect of depressing the value of T_{c1} both with respect to the MF and to the MHNC result. At the same time ρ_{c1} is displaced to larger value, with an increment of the order of 50% of the MF value (see table 2). Also with HRT one finds the second branch of fluid–fluid coexistence and a second critical point. The two coexistence curves for this second phase transition given by HRT and MF are very close to each other. On the other hand there is a significant difference in the region of the triple point. For $f = 32$ the temperature of the triple point is below T_{c2} by only 0.5% in the case of MF whereas it reaches 2% in the case of HRT. The difference is even more pronounced for $f = 24$. As already noted, in this case the second critical point in MF turns out to be metastable with respect to a transition which connects directly the low density branch of the first critical point and the high density branch. Therefore in this case there is no triple point at all in MF. This is not the case with HRT which gives a stable second critical point and a triple point, similar to the result for $f = 32$ but with a reduced range of the dip, the temperature of the triple point being 1.2% below T_{c2}. The smaller disparity between T_{c1} and T_{c2} should also be noted, T_{c1}/T_{c2} is equal to 1.88 for $f = 24$ and 2.48 for $f = 32$.

In a plot like that of figures 3 and 4 the coexistence curves given by MF and HRT look similar with only quantitative differences. It should be noted, however, that this is not completely true. Close to the critical temperatures the HRT curve is governed by a non-classical critical exponent $\beta = 0.345$ [18] whereas MF has the classical value $\beta = 1/2$ for the shape of the coexistence curve.

In summary all three theories give the same topology for the phase diagram with two critical points and a triple point and only minor quantitative differences are present. This peculiar behaviour is due to the ultrasoft logarithmic behaviour for $r < \sigma$. Some computation with a different set of values for the potential parameters A and B shows that the basic features of the phase diagram are not changed.

Table 2. Critical temperatures and densities for $f = 24, 32$ and parameters $A = 2.1\sigma$ and $B = 0.35\sigma$.

	ρ^*_{c1}	T^*_{c1}	ρ^*_{c2}	T^*_{c2}	ρ_{triple}	T_{triple}
$f = 32$						
MF	0.047	0.6722	1.960	0.2469	1.210	0.2460
MHNC	0.062	0.6230	1.960	0.2470		
HRT-SMSA	0.074	0.6123	1.952	0.2471	0.975	0.2426
$f = 24$						
MF	0.050	0.6700	1.920	0.3267		
MHNC	0.055	0.6600	1.900	0.327		
HRT-SMSA	0.084	0.6143	1.930	0.3268	0.986	0.3230

With respect to correlations we find that the effect of the attractive part $w(r)$ on the static structure factor $S(q)$ is significant in the small q region, the region of q where there is a direct link of $S(q)$ with the thermodynamics via the compressibility relation. At larger q values where $S(q)$ is a measure of the amount of short range order the effect of $w(r)$ is very small in the range of density of the phase transition.

5. Conclusions

We have studied a model of a fluid with a logarithmic repulsive interaction at short range and attractive forces at larger range. This interaction can model a solution of star polymers when dispersion forces are also relevant or depletion forces are present due to a third component. All three theories we have used (MF, MHNC and HRT) give qualitatively similar results: when the attraction becomes large enough two phase regions appear in the phase diagram but the peculiarity is that the line of first order phase transition bifurcates at a triple point into two lines terminating at two critical points. One of the critical points is at low density whereas the other is at large density where there is a strong overlap of the polymers. This second critical point is at a lower temperature than the first one. Only if the number of arms of the star polymer is less than 50 does this second branch correspond to a stable phase, otherwise it is pre-empted by a freezing transition. The low density branch of transition is rather similar to the standard liquid–vapour transition of a simple atomic fluid and it corresponds to a demodulate regime for the polymer solution. The high density branch on the other hand is specific to this model and it corresponds to a high concentration regime where there is a strong overlap of the star polymers. In this regime the basic role is played by the logarithmic part of the repulsive interaction and the effect of attraction in giving a second critical point is well represented by a mean-field contribution. Note, however, that the prediction of MF deviates significantly from the result of the RG liquid state theory HRT in the region of the triple point.

We note that other studies [26–28] have shown the existence of two critical points for models with a hard-core potential plus a soft repulsive shoulder and a long range attraction, an interaction advocated to be relevant for some simple atomic fluids. However for these models at most one of the two critical points turns out to be stable with respect to freezing.

At the high density of the second fluid–fluid transition one should worry about the possible presence of a glass transition. We have not investigated this possibility but this is a line of research well worth pursuing.

Acknowledgments

We thank Davide Pini for helpful discussions, and H Löwen, C N Likos and M Watzlawek who have made available their results (MC, RY) concerning the correlations for the model with the repulsive interaction.

Appendix. Integral equation for the radial distribution function

We have used the MHNC integral equation to compute the structure of star polymers solution in a good solvent modelled by the interatomic interaction $V_{rep}(r)$ equations (1) and (2). The MHNC equation starts from an exact relation [29], obtained from a cluster expansion, which connects the radial distribution function (rdf) $g(r)$ to the interparticle potential $V(r)$:

$$g(r) = \exp[-\beta V(r) + h(r) - c(r) + E(r)] \tag{13}$$

where $h(r) = g(r) - 1$ and $c(r)$ are the pair and the direct correlation function respectively. $c(r)$ is related to $h(r)$ by the Ornstein–Zernike equation

$$h(r) = c(r) + \rho \int c(|\boldsymbol{r} - \boldsymbol{r}'|)h(\boldsymbol{r}')\,\mathrm{d}\boldsymbol{r}'. \tag{14}$$

$E(r)$, called the *bridge function*, represents a sum of an infinite number of terms, the so-called *elementary* graphs in the diagrammatic analysis of the two-points function. The exact bridge function is not known for any system, equations (13) and (14) do not form a closed set of equations for a given $V(r)$ unless a closure is introduced for the bridge function.

In the MHNC scheme the *bridge function* of the system with potential $V(r)$ is replaced by the bridge function of a fluid of hard spheres of suitable diameter d. For hard spheres the correlations functions do not depend on the temperature but only on r/d and reduced density which can be expressed conveniently in term of the packing fraction $\eta_{HS} = (\pi/6)\rho d^3$. As diameter d of hard spheres we use the value determined by the so-called Lado criterion [21], i.e. the following equation must be satisfied

$$\int \mathrm{d}\boldsymbol{r}[g(r) - g_{HS}(r, \eta_{HS})]\frac{\partial E_{HS}(r, \eta_{HS})}{\partial \eta_{HS}} = 0. \tag{15}$$

This corresponds to the minimization of the Helmohtz free energy. As a bridge function of hard spheres we use the one deduced from equation (13) when the Verlet–Weis parameterization for g_{HS} is used [30]. This, together with equations (13)–(15), gives a closed set of equations which are solved by a standard iterative method.

When as the potential we use only the repulsive equations (1) and (2), the system under study is athermal, i.e. $\beta V_{rep}(r)$ does not depend on the temperature, so that the effective packing fraction η_{HS} entering into the bridge function does not depend on the temperature, but only on the functionality f of the star polymers and on the packing fraction $\eta = (\pi/6)\rho\sigma^3$, defined in terms of the diameter σ of the corona of the star polymer. It turns out that for any value of η equation (15) has a unique solution for η_{HS}.

The dependence of η_{HS} on the density as determined by equation (15) is peculiar (figure 5) and it reflects the features of the interparticle interaction. At low density η_{HS} is small and it increases rather quickly with the packing fraction. This reflects the fact that at these densities only the Yukawa part of $V_{rep}(r)$ (equation (2)) is relevant so that the system behaves like a standard soft core fluid. As η increases the rate of increase of η_{HS} diminishes until η_{HS} reaches a maximum (this happens for example, at $\eta \simeq 0.44$ for $f = 32$) as defined in section 1. Beyond such densities equation (1), is the relevant one. The ultrasoft character of the potential at short distances allows for a strong interpenetration between macroparticles, the amount of short

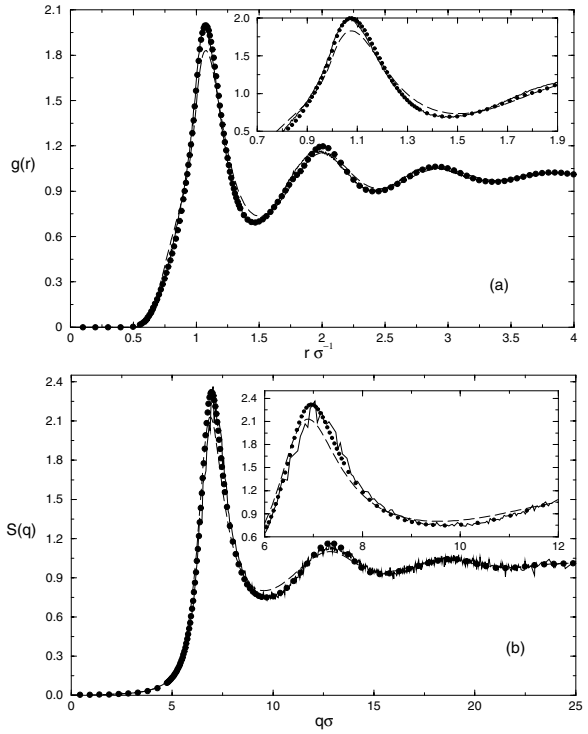

Figure A.1. (a) Comparison between the rdf obtained from the MC simulation (solid curve) and the MHNC (circles) and RY (dashed curve) closures for $f = 32$ and $\eta = 0.60$ ($g(r)$ versus reduced distance r/σ). (b) Comparison between the structure factors obtained from the MC simulation and the MHNC and RY closures for $\eta = 0.60$ ($S(q)$ versus $q\sigma$). In both cases the inset shows a detail of the main figure.

range order diminishes and the effective HS diameter of the bridge function decreases as the density increases. At still larger packing fractions there is a turn over and a new maximum of η_{HS} at $\eta \simeq 3.1$ for $f = 32$. Beyond this value the dominant peak of $S(k)$ (which was the second peak at small densities) begins to decrease, testifying to a re-entrant loss of the spatial ordering of the stars. A similar non-monotonic dependence of η_{HS} on η is common to other values of f.

Considering the evolution of the height of the main peak of $g(r)$, when the density varies, we have seen that this evolution follows the anomalous one of the structure factor main peak.

For this system extensive simulation results are available [6] and we find that there is an excellent agreement with the MHNC results. For most of the densities $g(r)$ and $S(q)$ are essentially indistinguishable from the simulation results and are not shown here. Some small deviations are present in the region of strongest coupling, i.e. in the density regions where η_{HS} has a maximum. As an example the results for $f = 32$ and for two densities in these regions, $\eta = 0.60$ and 3.14, are shown in figures A.1 and A.2. One can also appreciate that in these regions the MHNC is quite accurate.

Another integral equation has been used to study the correlations for this model system, the RY equation. For most density values this equation also reproduces the simulation data very well at the level of the MHNC. However in certain density ranges significant deviations from simulation are present. For $f = 32$ this happens at $0.2 \leqslant \eta < 0.8$ and in the region

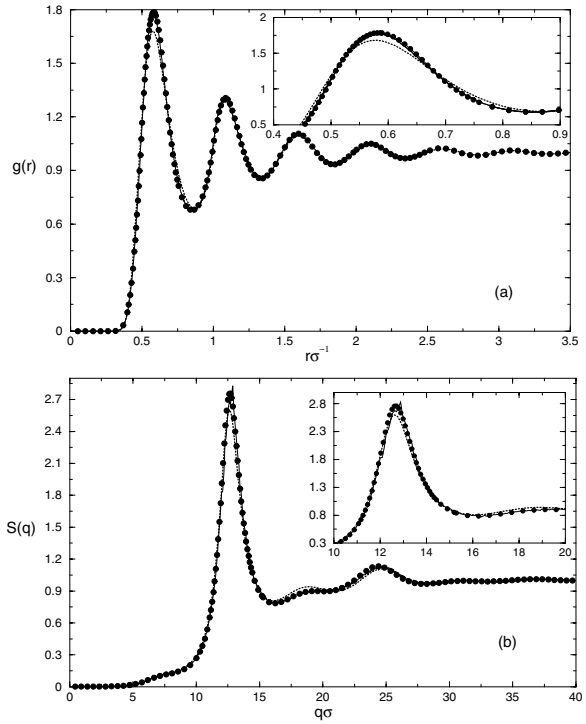

Figure A.2. (a) Comparison between the radial distribution functions obtained from MC simulation (solid curve) and the MHNC (circles) and RY (dashed curve) closures for $f = 32$ and $\eta = 3.14$ ($g(r)$ versus r/σ). (b) Comparison between the structure factors obtained from MC simulation and the MHNC and RY closure $\eta = 3.14$ ($S(q)$ versus $q\sigma$). The density is near the value for which the first peak has completely disappeared and the second peak is the main one. In both cases the inset shows a detail of the main figure.

around $\eta = 3$, the density ranges of strongest coupling. Also the RY results are plotted in figures A.1 and A.2 and one can appreciate the improvement that the MHNC represents compared to RY. We conclude that the MHNC is also very accurate for ultrasoft repulsive interactions and this gives additional evidence for the universality of the bridge function. The MHNC results for $V_{rep}(r)$ has been used to obtain the equation of state by integrating over density the compressibility given by $S(0)$ and this appears in the MF analysis of section 2. The same MHNC results have also been used as an initial condition in the HRT computation of section 3.

References

[1] Pusey P N 1948 *Colloidal Suspension (Les Houches Session Series)* ed J P Hansen, D Levesque and J Zinn Justin (Amsterdam: Elsevier)
[2] Likos C N, Schmidt M, Löwen H, Ballauff M, Pötschke D and Lindner P 2001 *Macromolecules* **34** 2914
[3] Likos C N, Rosenfeldt S, Dingenouts N, Ballauff M, Lindner P, Werner N and Vögtle F 2002 *J. Chem. Phys.* **117** 1869
[4] Bolhuis P G, Louis A A, Hansen J P and Meijer E J 2001 *J. Chem. Phys.* **4** 4296
[5] Witten T A and Pincus P A 1986 *Macromolecules* **19** 2509
[6] Watzlawek M, Löwen H and Likos C N 1998 *J. Phys.: Condens. Matter* **10** 8189
[7] Watzlawek M, Likos C N and Löwen H 1999 *Phys. Rev. Lett.* **82** 5289

[8] Groh B and Schmidt M 2000 *J. Chem. Phys.* **114** 5450
[9] Dozier W D, Huang J S and Fetters L J 1991 *Macromolecules* **24** 2810
[10] Willner L, Jucknischke O, Richter D, Roovers J, Zhou L-L, oporowski P M, Fetters L J, Huang J S, Lin M and Hadjichristidis N 1994 *Macromolecules* **27** 3821
[11] Grest G S, Fetters L J, Huang J S and Richter D 1996 *Adv. Chem. Phys.* **94** 67
[12] Likos C N, Löwen H, Watzlawek M, Abbas Jucknischke O, Allgaier J and Richter D 1998 *Phys. Rev. Lett.* **80** 4450
[13] Rogers F J and Young D A 1984 *Phys. Rev.* A **30** 999
[14] Zerah G and Hansen J-P 1986 *J. Chem. Phys.* **84** 2336
[15] Lang A, Kahl G, Likos C N, Löwen H and Watzlawek M 1999 *J. Phys.: Condens. Matter* **11** 10143
[16] Lado F, Foiles S M and Ashcroft N W 1983 *Phys. Rev.* A **28** 2374
[17] Parola A and Reatto L 1984 *Phys. Rev. Lett.* **53** 2417
Parola A and Reatto L 1985 *Phys. Rev.* A **31** 3309
[18] Parola A and Reatto L 1995 An ample review of HRT is contained in *Adv. Phys.* **44** 211
[19] Daoud M and Cotton J P 1982 *J. Physique* **43** 531
[20] Jusufi A, Dzubiella J, Likos C N, von Ferber C and Löwen H 2001 *J. Phys.: Condens. Matter* **13** 6177
[21] Lado F 1982 *Phys. Rev. Lett.* A **89** 196
[22] Rosenfeld Y, Schmidt M, Watzlawek M and Löwen H 2000 *Phys. Rev.* E **62** 5006
[23] Likos C N and Harreis H M 2002 *Condensed Matter Phys.* **5** 173
[24] Likos C N, Hoffman N, Löwen H and Louis A A 2002 *J. Phys.: Condens. Matter* **14** 7681
[25] Barocchi F, Chieux P, Fontana R, Magli R, Meroni A, Parola A, Reatto L and Tau M 1997 *J. Phys.: Condens. Matter* **9** 8849
[26] Malescio G and Pellicane G 2001 *Phys. Rev.* E **63** 020501/1
[27] Jagla E A 1999 *J. Chem. Phys.* **111** 8980
[28] Franzese G, Malescio G, Skibinsky A, Buldyrev S V and Stanley H E 2001 *Nature* **409** 692
[29] Hansen J P and McDonald I R 1986 *Theory of Simple Liquids* (London: Academic)
[30] Verlet L and Weis J-J 1972 *Phys. Rev.* A **5** 939